Article

Kinetic Aspects of Suzuki Cross-Coupling Using Ligandless Pd Nanoparticles Embedded in Aromatic Polymeric Matrix

Valentin N. Sapunov [1], Linda Z. Nikoshvili [2,*], Elena S. Bakhvalova [3], Mikhail G. Sulman [2] and Valentina G. Matveeva [2]

[1] Department of Chemical Technology of Basic Organic and Petrochemical Synthesis, D. Mendeleev University of Chemical Technology of Russia, Miusskaya pl., 9, 125047 Moscow, Russia; sapunovvals@gmail.com

[2] Department of Biotechnology, Chemistry and Standardization, Tver State Technical University, A. Nikitina Str., 22, 170026 Tver, Russia; sulmanmikhail@yandex.ru (M.G.S.); matveeva@science.tver.ru (V.G.M.)

[3] Regional Technological Centre, Tver State University, Zhelyabova Str., 33, 170100 Tver, Russia; bakhvalova.es@mail.ru

* Correspondence: nlinda@science.tver.ru; Tel.: +7-904-005-7791

Abstract: During the last decades, palladium nanoparticles (Pd(0) NPs) and Pd(II) compounds were shown to be attractive catalysts for fine organic synthesis. Nanostructured Pd(0) or Pd(II) catalysts have a relatively low environmental impact, but, at the same time, they are indispensable for such processes as Suzuki cross-coupling. This paper describes the preparation of Pd(0) or Pd(II) supported/embedded in hyper-cross-linked polystyrene (HPS) and compares their activity in Suzuki cross-coupling between phenylboronic acid and 4-bromoanisole. Obviously, the palladium charge (Pd(0) ↔ Pd(II)) changes continuously during the reaction catalytic cycle. It would seem that the use of the starting palladium in the form of Pd(0) or Pd(II) should not affect the reaction's kinetic laws for both catalysts, but their special individuality is manifested between them. Nanoparticulate Pd(0) catalysts are stable during the reaction. In contrast, catalysts based on Pd(II) are extremely active in the initial period of the reaction, but then the "hot form" of the catalyst is rapidly converted into the form of Pd(0), whose activity is identical to that of the preliminarily reduced catalyst. This work discusses the possible nature of this phenomenon. A mathematical model for Suzuki cross-coupling reaction was suggested that was able to adequately describe experimental data. The level of reliability (R^2) of the correlation between the experimental and calculated data was $R^2 = 0.97–0.99$.

Keywords: Suzuki cross-coupling; palladium; hyper-cross-linked polystyrene; phenylboronic acid; 4-bromoanisole

1. Introduction

Pd-catalyzed reaction of Suzuki cross-coupling between aryl halides and arylboronic acids is a versatile and industrially important tool for the synthesis of biaryls, which are intermediates of different active pharmaceutical ingredients (APIs), ligands, and polymers [1–4]. The generally accepted mechanism of the Suzuki reaction involves the oxidative addition of aryl halide to the active Pd(0) atom, followed by the transfer of an aryl group from boronic acid to the Pd(II) center (transmetalation) [5,6]. Reductive elimination is the final stage of the catalytic cycle, which gives the target cross-coupling product and also regenerates the palladium catalyst so that it can again participate in the catalytic cycle [7]. In addition, arylboronic acid's homo-coupling products can accumulate in the reaction mixture. This mechanism was confirmed for homogeneous Pd complexes, which are traditional Suzuki cross-coupling catalysts [8–10].

Obviously, heterogeneous (and particularly supported) Pd catalysts are of particular interest for the industrial production of pharmaceuticals. A lot of research efforts are devoted towards the replacement of homogeneous catalysts by their heterogeneous

analogs, which allow recycling, easy separation, and the possibility of continuous processing, resulting in process intensifications [11,12]. However, it should be noted that the use of transition metals in organic synthesis is limited by some critical disadvantages, such as their high cost, toxicity, leaching of catalytically active metal forms, and necessity of their capture, which significantly limit their practical applicability, especially in the pharmaceutical industry [13–16].

In order to increase the durability and reusability of heterogeneous catalysts, the most significant factor is the choice of a suitable, safe, and stable support. We recently demonstrated that Pd nanoparticles (NPs) confined in hyper-cross-linked polystyrene (HPS) can be used as a Suzuki cross-coupling catalyst [17]. The developed Pd/HPS catalyst was found to be highly effective in the cross-coupling of 4-bromoanisole (BrAn) and phenylboronic acid (PBA). For this catalyst, the change in Pd NPs' distribution after catalytic experiments took place due to Pd reprecipitation in the internal volume of the polymeric matrix, which nevertheless did not result in catalyst deactivation [17]. Indeed, the results of numerous studies of the Suzuki cross-coupling show that several forms of palladium can simultaneously participate in the catalytic cycle: dissolved molecular complexes Pd(0) and Pd(II), colloidal Pd in solution and/or on a support, and large-diameter particles of metallic palladium. It is assumed that these forms of the catalyst mutually transform into each other during the reaction [18,19]. Thus, various processes (e.g., aggregation, dissociation, leaching, etc.) can contribute to changes in the catalyst morphology and, as a result, its activity and selectivity [20–24].

For heterogeneous (or "ligandless") Pd-containing catalysts, two mechanisms were proposed [25,26]: heterogeneous (when palladium atoms with a low coordination number in the NPs are responsible for the catalytic activity, and the adsorption of aryl halide on the NP surface is a necessary step) and homogeneous (when dissolved palladium is the most active [27]). Depending on the type of palladium compound in the catalyst composition (Pd(II) species or Pd(0) NPs), one of the above two mechanisms may prevail. It is important to emphasize that, for ligandless Pd-containing catalysts containing Pd NPs as a source of catalytically active species, the reaction elementary steps are the same as for homogeneous complexes, However, the observed kinetics, as well as the interpretation of the results of single catalytic experiments, are complicated by the existence of different forms of Pd in the catalyst composition or/and in the solution (Figure 1).
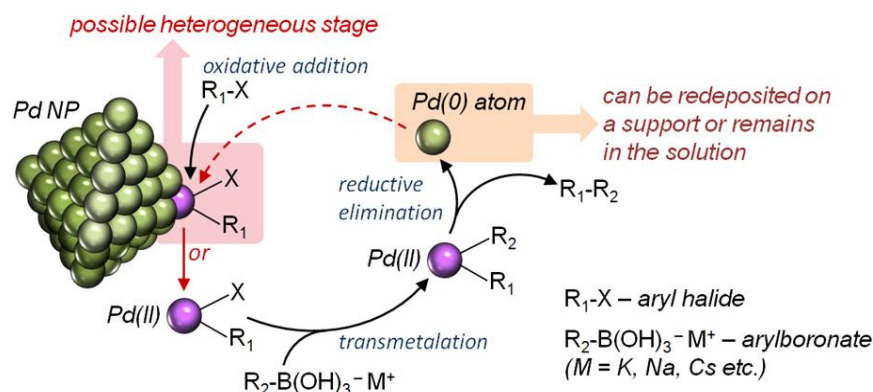

Figure 1. Simplified scheme of Suzuki cross-coupling in the presence of nanoparticulate ligandless catalyst involving both heterogeneous and homogeneous stages.

All the factors mentioned above make it difficult to study the kinetics of Suzuki cross-coupling using ligandless catalysts. There are a very limited number of studies devoted to the kinetics of cross-coupling reactions [28–31]. To the best of our knowledge, there are no data in the literature on the kinetics studies of the Suzuki reaction in the presence of ligandless catalysts based on polymer-encapsulated Pd NPs.

This work is devoted to the study of the kinetic peculiarities of the Suzuki reaction by the example of cross-coupling of BrAn and PBA using a ligandless Pd/HPS catalyst

containing welldefined Pd NPs. Assuming the multiple short-lived forms of Pd existing in situ as well as the fact that, in the case of a Pd/HPS catalyst, the reaction occurs in the pores of the HPS and no leaching of Pd was found in this work, for the first time, a formal kinetic approach was applied to describe the behavior of a ligandless catalyst for Suzuki cross-coupling based on HPS [17]. Moreover, the objective of this work is to show the possibility of the application of "non-formal kinetics" methods to study complex multi-step catalytic processes, such as Suzuki cross-coupling.

2. Materials and Methods

2.1. Materials

HPS Macronet MN270 (Purolite Int., Llantrisant, UK) was washed with distilled water and acetone and dried under vacuum as described elsewhere [32]. 4-Bromoanisole (BrAn, ≥98%) was purchased from Merck KGaA, Darmstadt, Germany. 4-Methoxybiphenyl (MBP, >99%) was purchased from Tokyo Chemical Industry Co. Ltd, Tokyo, Japan. Phenyl-boronic acid (PBA, 95%), diphenylamine (99%), biphenyl (BP, 99.5%), tetrahydrofuran (THF, ≥99.9%), ethanol (EtOH, ≥99.8%), isopropanol (i-PrOH, ≥99.5%), sodium hydroxide (NaOH, ≥98%), sodium carbonate (Na_2CO_3, ≥99.5%), and potassium carbonate (K_2CO_3, ≥99.0%) were obtained from Sigma-Aldrich, St. Louis, MO, USA. Palladium acetate ($Pd(CH_3COO)_2$, Pd content 47.68%) was purchased from JSC "Aurat" (Moscow, Russia). All chemicals were used as received. Distilled water was purified with an Elsi-Aqua water purification system.

2.2. Analysis Tools

2.2.1. Gas Chromatography-Mass Spectrometry

In each catalytic experiment, samples of the reaction mixture were periodically taken and analyzed via GC-MS (Shimadzu GCMS-QP2010S) equipped with a capillary column HP-1MS (100 m × 0.25 mm i.d., 0.25 μm film thickness). Helium was used as a carrier gas at a pressure of 74.8 kPa and a linear velocity of 36.3 cm/s. Oven temperature was programmed as follows: 120°C (0 min) → 10 °C/min (160 °C) → 25 °C/min (300 °C) → 300 °C (2.4 min). The temperature of the injector, interface, and ion source was 260 °C, with a range of 10–500 m/z. The concentrations of the reaction mixture components were calculated using the internal standard calibration method (diphenylamine was used as an internal standard). It is noteworthy that, during the GS-MS analysis, PBA underwent dehydration and trimerization, which negatively affected the signal intensity. Thus, due to the low level of confidence in the quantitative analysis of PBA content, the kinetics of its consumption was not studied.

2.2.2. X-ray Fluorescence Analysis

X-ray fluorescence analysis (XFA) was carried out to determine the Pd content. It was performed with a Zeiss Jena VRA-30 spectrometer (Mo anode, LiF crystal analyzer, and SZ detector). Analyses were based on the Co Kα line and a series of standards prepared by mixing 1 g of polystyrene with 10–20 mg of standard compounds. The time of data acquisition was constant at 10 s.

2.2.3. X-ray Photoelectron Spectroscopy

X-ray photoelectron spectroscopy (XPS) data were obtained using Mg Kα (hν = 1253.6 eV) radiation with the ES-2403 spectrometer (Institute for Analytical Instrumentation of the RAS, St.Petersburg, Russia) equipped with an energy analyzer PHOIBOS 100-MCD5 (SPECS, Berlin, Germany) and a X-ray source XR-50 (SPECS, Berlin, Germany). All the data were acquired at a X-ray power of 250 W. Survey spectra were recorded at an energy step of 0.5 eV with an analyzer pass energy of 40 eV, and high-resolution spectrum were recorded at an energy step of 0.05 eV with an analyzer pass energy of 7 eV. Samples were allowed to outgas for 180 min before analysis and were stable during the examination. The data analysis was performed by CasaXPS.

2.2.4. Scanning Transmission Electron Microscopy

Scanning Transmission Electron Microscopy (S/TEM) characterization was carried out using the FEI Tecnai Osiris instrument (Thermo Fisher Scientific, Waltham, MA, USA) operating at an accelerating voltage of 200 kV, equipped with a HAADF detector (Fischione, Export, PA, USA) and an EDX microanalysis spectrometer (EDAX, Mahwah, NJ, USA). Samples were prepared by embedding the catalyst in epoxy resin with subsequent microtomming (ca. 50 nm thick) at ambient temperature. For the image processing Digital Micrograph (Gatan, Pleasanton, CA, USA) software and TIA (Thermo Fisher Scientific, Waltham, MA, USA) were used. Holey carbon/Cu grid was used as a sample support.

2.3. Experimental Procedures

2.3.1. Catalysts Preparation

Pd-containing HPS-based catalyst (Pd content: 2.5 wt.%, XFA data) was synthesized via the wet-impregnation method. In a typical experiment, 1 g of pretreated, dried, and crushed (<63 μm) HPS granules were impregnated with 2.8 mL of the THF solution of precursor (Pd(CH$_3$COO)$_2$) of a certain concentration. The Pd-containing polymer was dried at 70 °C until a constant weight was achieved (designated as Pd(II)/HPS). After that, the catalyst was reduced in a hydrogen flow (100 mL/min) at 300 °C for 3 h (designated as Pd(0)/HPS).

It is noteworthy that, for the kinetic study, we have chosen this type of catalyst, i.e., one synthesized on the base of non-functionalized HPS of MN270-type in order to avoid the possible contribution of functional groups of the polymeric support. At the same time, the use of Pd acetate allowed excluding the influence of residual chloride ions, since it is known that PdCl$_2$ or other Cl-containing metal precursors cannot be completely reduced in the polymeric matrix during the treatment with molecular hydrogen at 300 °C [33]. Moreover, palladium acetate has a high affinity for the hydrophobic polymeric environment during the impregnation process due to its ability to form trimers in THF [34].

2.3.2. Reaction Procedure

Testing of a Pd-containing HPS-based catalyst was performed in a 60 mL shaker-type isothermal glass batch reactor with vigorous stirring. The total volume of the liquid phase was 30 mL. Mixture of EtOH and water was used as a solvent. The choice of an EtOH/water mixture was caused, on the one hand, by the environmental safety of these solvents and, on the other hand, by the absence of necessity to use phase-transfer agents, since the system remained homogeneous in the range of selected concentrations of the starting reagents (BrAn, PBA, and NaOH) and the resulting products (MBP and BP). Moreover, protic solvent systems were proven to be beneficial in the Suzuki reaction [35].

The Suzuki cross-coupling was performed with variations in the following reaction parameters: Pd concentration (0.157 mmol/L, 0.235 mmol/L or 0.392 mmol/L, which are equivalent to 0.47 mol.%, 0.70 mol.% or 1.17 mol.% with respect to BrAn, respectively), PBA amount (1.5 mmol or 2.0 mmol), NaOH amount (1.5 mmol or 2.0 mmol), BrAn amount (0.5 mmol, 1.0 mmol or 2.0 mmol), stirring intensity (400, 600, and 800 two-sided shaking per minute), reaction temperature (40–70 °C), EtOH-to-H$_2$O ratio (volumetric ratio: 2:1 or 5:1) and base (NaOH, Na$_2$CO$_3$ or K$_2$CO$_3$). The excess of PBA with respect to BrAnwas used in most cases due to the possible non-selective catalyst behavior as a result of PBA homocoupling with the formation of the side product—BP.

Before adding the catalyst to the reactor, in each experiment, the blank test was carried out (the reaction mixture was heated for 60 min and analyzed) to ensure that the reaction does not proceed in the absence of catalyst.

Preliminary experiments showed that the cross-coupling reaction of these reagents proceeds almost quantitatively (97–99 mol.%); the formation of BP does not exceed 2 mol.%, and the formation of σ,σ′-dianisoles is not detected. The data obtained make it possible to study this reaction in more detail.

3. Results

3.1. Catalyst Characterization

Synthesized Pd(0)/HPS was analyzed by the XPS and S/TEM. It was found that Pd(0)/HPS contains numerous palladium NPs with a mean diameter of 8.2 ± 2.4 nm located in the HPS' pores (Figure 2). According to the XPS data, the following values of binding energy of Pd $3d_{5/2}$ were found [36]: 335.0 eV (metallic Pd), 336.3 eV (partially oxidized NPs PdO/Pd), and 337.2 eV (PdO). The presence of Pd(II) on the surface of the preliminarily reduced HPS-based sample was due to the fact that the catalyst was stored in air.
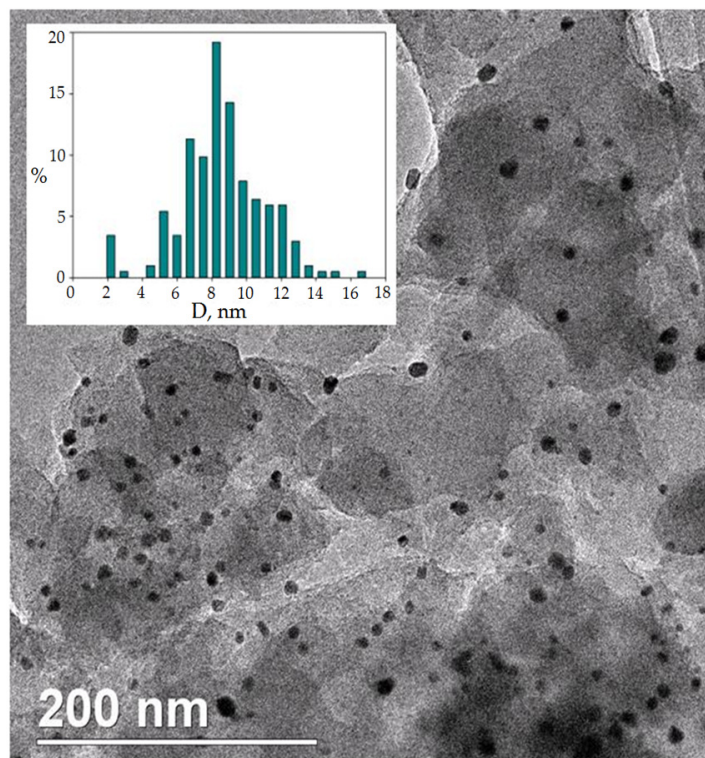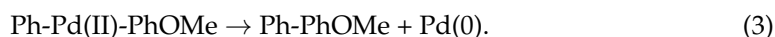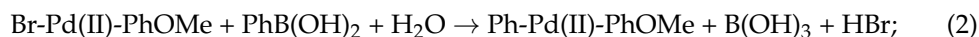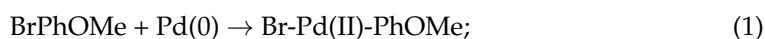

Figure 2. S/TEM image of Pd(0)/HPS.

### 3.2. Effect of PBA-to-NaOH Ratio

The amount of PBA and NaOH taken for the Suzuki reaction, as well as their molar ratio, are very important parameters, often limiting the conversion of aryl halides. Indeed, without adding a base, the reaction does not proceed. If we take half as many bases as PBA, the reaction stops at about 50% BrAn conversion.

Formally, the reaction scheme can be presented in the form of sequential reactions:

$$BrPhOMe + Pd(0) \rightarrow Br\text{-}Pd(II)\text{-}PhOMe; \tag{1}$$

$$Br\text{-}Pd(II)\text{-}PhOMe + PhB(OH)_2 + H_2O \rightarrow Ph\text{-}Pd(II)\text{-}PhOMe + B(OH)_3 + HBr; \tag{2}$$

$$Ph\text{-}Pd(II)\text{-}PhOMe \rightarrow Ph\text{-}PhOMe + Pd(0). \tag{3}$$

As a result of the reactions, a strong mineral acid should be formed as one of the products capable of destroying all palladium complexes, and reaction (3) cannot proceed. The strong acid must be neutralized. The idea of neutralizing HBr was realized by converting PBA into a salt form, that is, into a cation and tetrahedral anion $[PhB(OH)_3]^-$ [5,37,38]. The phenyl group in the anion acquires a certain electron density, thereby facilitating the transmetalation reaction. It is clear that, as this reaction proceeds, the phenylboronic anion is destroyed, and the base is neutralized to form NaBr. In more detail, we will consider the process of transfer of the phenyl fragment to a positively charged palladium atom later

(Section 3.3.5). Since PBA is very weak (pK = 8.83), the equilibrium formation of the above salt is not completely shifted to the right:

$$PhB(OH)_2 + NaOH \leftrightarrow Na^+ \, [PhB(OH)_3]^-. \tag{4}$$
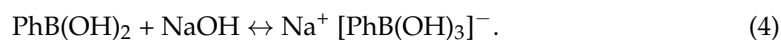
The concentration of an active carrier of the phenyl group is not sufficient for the complete conversion of aryl halide. This circumstance is the reason that for the complete conversion of BrAn the molar ratio [BrAn]:[PBA]:[NaOH] should not be equimolar; there should be more of the alkaline component. Based on the results of additional experiments, we have chosen the stated molar ratio as 1.0:1.5:1.5, respectively, and this ratio was used in subsequent experiments. A further increase in the excess amount of the sodium salt of PBA does not lead to a significant change in either the rate of formation of BrAn or the formation of a by-product, biphenyl.

With the use of the initial Pd(II)/HPS catalyst, a further increase in the amount of NaOH from 1.5 mmol up to 2.0 mmol (Figure 3a) at a constant PBA content (1.5 mmol) allowed increasing the BrAn conversion in 60 min from 90.4% up to 98.3%. In spite of the statements [37–39] that the borate pathway (formation of poorly reactivetrihydroxyborate in the presence of a sufficiently strong base) is competitive with the hydroxo pathway, it is also obvious that it cannot be extrapolated to all the catalytic systems and that the molar excess of NaOH is beneficial for HPS-based Pd-containing catalysts.
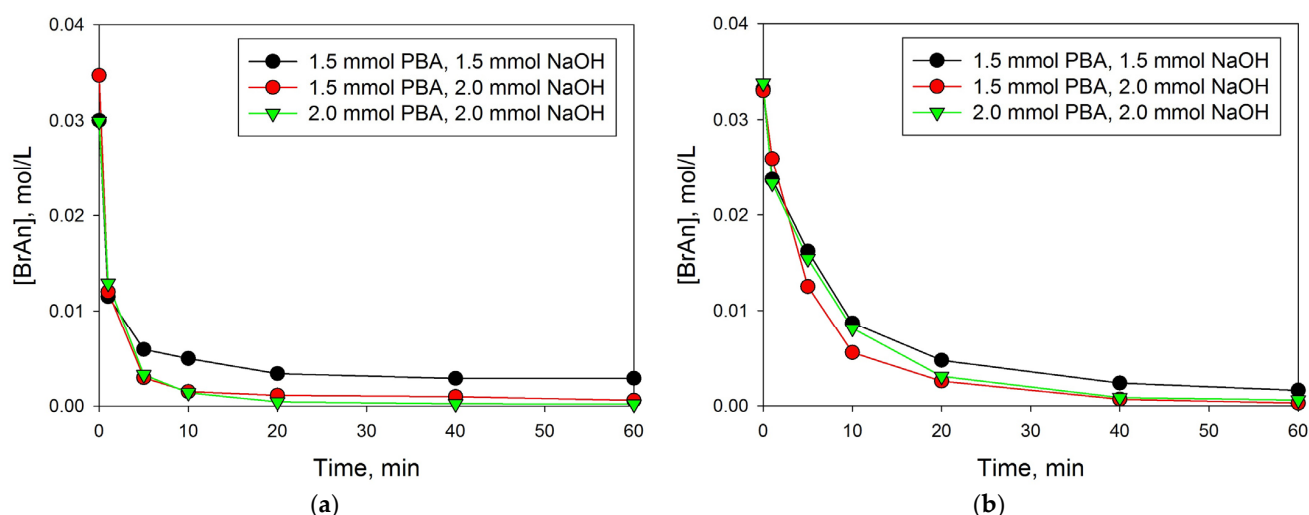

Figure 3. Influence of PBA-to-NaOH ratio on the activity of initial Pd(II)/HPS (**a**) and reduced Pd(0)/HPS (**b**) catalyst (0.47 mol.% Pd, 1 mmol BrAn, EtOH/H$_2$O = 5:1, 60 °C, N$_2$, 800 two-sided shaking/min).

The increase in PBA amount up to 2.0 mmol (at 2.0 mmol of NaOH) allowed a further increase in BrAn conversion up to 99.4%. (Figure 3a). The excess in PBA was due to the fact that BP was formed as a side product, while NaOH, as mentioned above, reacted with both HBr and PBA.

In the case of Pd(0)/HPS, the increase in NaOH amount from 1.5 mmol up to 2.0 mmol at 1.5 mmol of PBA (Figure 3b) also resulted in an increase in BrAn conversion from 96.4% up to 99.2% for 60 min. However, in contrast to Pd(II)/HPS, the increase in PBA amount up to 2.0 mmol did not provide the reaction acceleration. Thus, for Pd(0)/HPS, the PBA-to-NaOH ratio 1.5:2.0 was chosen as optimal.

As expected, the replacement of alkali (NaOH) by weaker bases (K$_2$CO$_3$ or Na$_2$CO$_3$) did not lead to deep BrAn conversions (Figure 4).
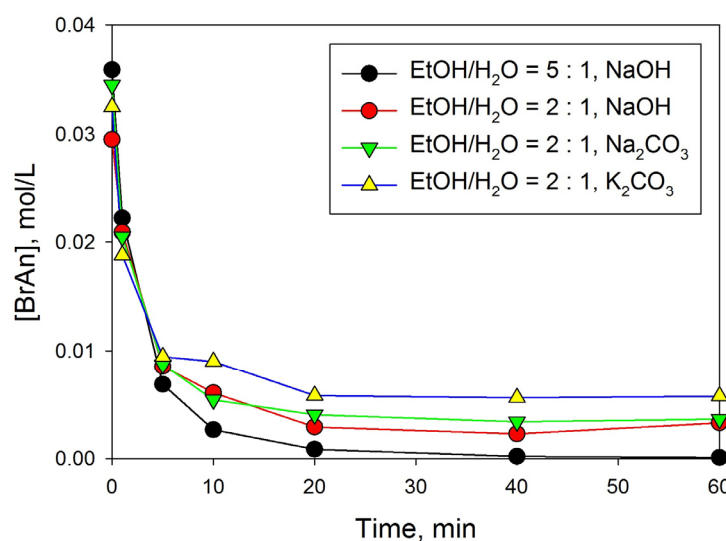
Figure 4. Influence of EtOH-to-H$_2$O ratio and base on the activity of reduced Pd(0)/HPS (0.47 mol.% Pd, 1 mmol BrAn, 1.5 mmol PBA, 2 mmol of base, 70 °C, N$_2$, 800 two-sided shaking/min).

3.3. Kinetic Studies and Modeling

Kinetic studies were carried out in several series of experiments, in each of which only one parameter was changed, if possible. The series were as follows:

(i) Influence of the catalyst amount (Pd(II)/HPS or Pd(0)/HPS) on the reaction rate at constant initial concentrations of other components: 1 mmol BrAn, 1.5 mmol PBA, and 1.5 mmol NaOH (EtOH/H$_2$O = 5:1, 60 °C, N$_2$, 800 two-sided shaking/min);

(ii) Influence of the initial concentration of BrAn ([BrAn]$_0$) while maintaining the initial molar ratio of BrAn-to-PBA and NaOH (EtOH/H$_2$O = 5:1, 60 °C, N$_2$, 800 two-sided shaking/min);

(iii) Influence of temperature on the activity of a reduced Pd(0)/HPS catalyst (0.47 mol.% Pd, 1 mmol BrAn, 1.5 mmol PBA, 2 mmol NaOH, EtOH/H$_2$O = 5:1, N$_2$, 800 two-sided shaking/min).

However, before starting the study of the kinetics of the reaction, it was necessary to decide the question of the possible influence of diffusion processes on the reaction rate.

3.3.1. Diffusion Effect

The reaction mass includes a heterogeneous catalyst and a liquid reaction medium, which, in principle, can be transformed into a two-phase system. To ensure that there were no external diffusion limitations, the effect of stirring intensity on the Suzuki reaction between BrAn (1 mmol) and PBA (1.5 mmol) was investigated for a pre-reduced sample of Pd(0)/HPS catalyst. The reaction was carried out at 60 °C under a nitrogen atmosphere using 2.0 mmol NaOH and 400–800 two-sided shaking/min. The progress of the reaction was monitored by the consumption of the starting BrAn. The kinetic curves were found to be superimposed on one another in the range of 600–800 two-sided shaking/min (Figure S1), indicating the identity of the processes and the independence of the reaction rate from hydrodynamic conditions. In other words, there is no diffusion inhibition of the studied processes.

3.3.2. Influence of the Amount of Catalysts

We will study the effect of the amount of catalyst using the "time transformation" method, the essence of which is to compare the kinetic curves with each other in a series of one-factor experiments [40]. In such a series of experiments, only the concentration or amount of the catalyst changes, all other parameters being equal (temperature, initial concentration of the reagent, solvent, etc.). The kinetic equation for the consumption of

the main reagent, BrAn, in the presence of the catalyst $[cat]_i$ can be represented as follows (Equation (5)):

$$d[BrAn]\Big/dt = -[cat]_i \cdot f([BrAn], T, \ldots \ldots) \tag{5}$$

As a rule, the kinetic data of such a series are a fan of curves originating from a point on the ordinate axis, which corresponds to the initial concentration of the measured reagent (in our case, it is $[BrAn]_0$). The necessary condition is an equality of the initial concentrations of the reagent. One of these curves can be considered for comparison. Let us call this experiment a comparison experiment, and the amount of catalyst in this experiment is $[cat]_0$. In this particular case, $[cat]_0 = 1.17$ mol.% of Pd(0)/HPS catalyst.

The next step in considering the selected series of experiments is the transformation of Equation (5) into Equation (6).

$$d[BrAn]\Big/dt = -\lambda \cdot [cat]_0 \cdot f([BrAn], T, \ldots \ldots) \tag{6}$$

where the coefficient λ is the ratio

$$\lambda = [cat]_i \Big/ [cat]_0 \tag{7}$$

Based on the assumption that the ratio of catalysts is involved as a factor in the rate equation and is not a function of time (the catalyst is stable during the reaction), the rate equation in integral form has the form of Equation (8):

$$\int_{[BrAn]_0}^{[BrAn]_i} \left([BrAn] \Big/ [cat]_0 \cdot f([BrAn], \ldots \ldots) \right) = -\lambda \cdot t \tag{8}$$

where $[BrAn]_0$ and $[BrAn]_i$ are the initial and current concentrations of BrAn; (t) is the reaction time; (λ) is the ratio of the compared amounts of catalysts; (λ t)—"reduced" or "conditional" reaction time.

The right side of Equation (8) is the experimental values of the concentration $[BrAn]i$ for the reaction under catalysis $[cat]_0$ at the time point (t), i.e., for the case $\lambda = 1$. For all other experiments in this series of experiments with catalysts $[cat]_i$, the numerical value (λ) can be adjusted so that the corresponding concentration values of the $[BrAn]_i$ overlap with the trend line of the corresponding values of the comparative experiment.

Thus, all data from a series of one-factor experiments with a change in the amount of Pd(0)/HPS catalyst on the plot of $[BrAn]_i$ vs. (λ t) represent a single diagram with one trend line (Figure 5).

For the series of experimental data obtained at variations of the reaction temperature, PBA-to-NaOH ratio, and catalyst loading, with the exclusion of some experiments where limitation of the reaction rate was found, the residual sum of squares (*RSS*) for the proposed kinetic model was equal to 7.77×10^{-5}, the variance was equal to 2.51×10^{-6}, and the standard deviation (*SD*) was 1.61×10^{-3}.

Theoretically, the numerical value of the coefficient (λ) should be equal to the ratio of catalyst amounts (Equation (7)), which we will refer to as λ(calc). However, the obtained coefficient λ(exp), at which the current $[BrAn]i$ concentrations of other experiments were superimposed on the trend line of the comparative experiment, does not correspond to the calculated one, although there is a linear relationship between them (Figure 6).

In this regard, let us analyze the discrepancy between the calculated and experimental coefficients λ when analyzing the kinetic data for the Pd(0)/HPS catalyst. The underestimated value of λ(exp) indicates that not all of the palladium in the catalyst is involved in the catalytic condensation of BrAn and PBA. For example, the proportion of active palladium with a minimum amount is about half.
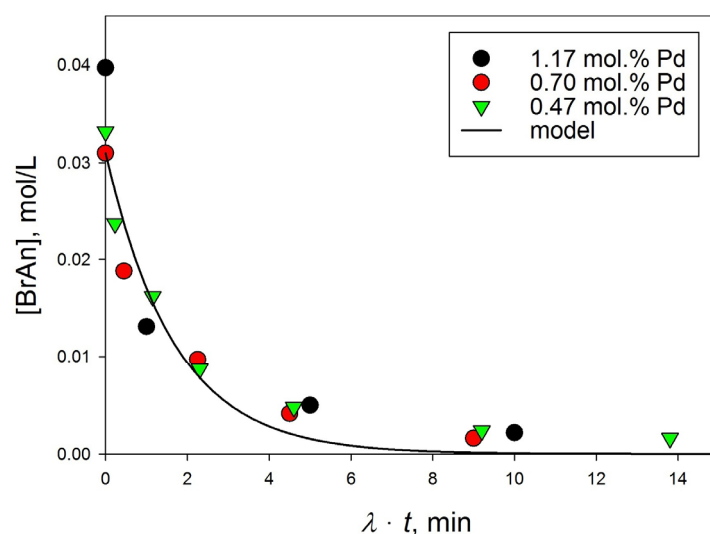
Figure 5. Dependence of the current concentration of BrAn on "conditional" reaction time in a series of experiments with different amounts of Pd(0)/HPS catalyst (black circle—1.17 mol.%, red circle—0.70 mol.%, green triangle—0.47 mol.%); the line is the calculated curve according to the model (see Section 3.3.5).
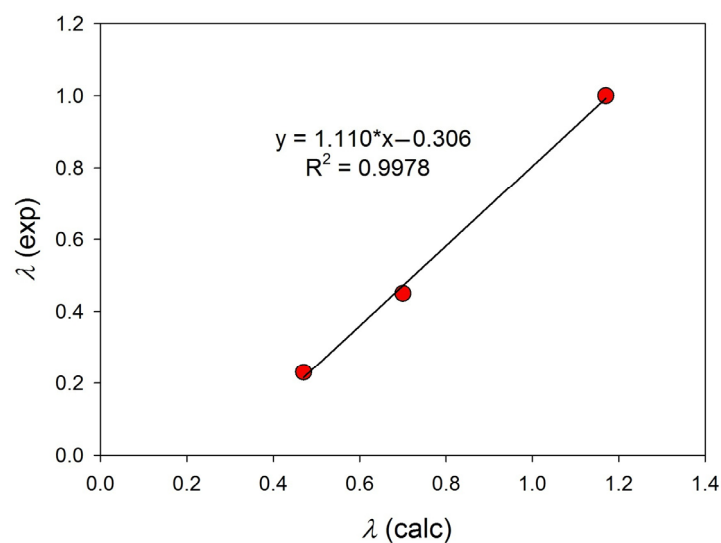

Figure 6. Correlation of calculated and experimental reduced time transformation coefficients.

Thus, either the total surface area with active palladium particles has decreased, or the large palladium particles in the HPS matrix are not available to other agents. The second assumption is most likely, since the same amount of palladium is blocked for all the catalysts taken, as shown by the diagram in Figure 6. This phenomenon can be explained by the results of S/TEM analysis (Figure 2), which show that, in the Pd(0)/HPS sample, there are numerous palladium NPs with a mean diameter of 8.2 ± 2.4 nm, located in the pores of the HPS (see Section 3.1).

Carrying out the same analysis with a series of Pd(II)/HPS catalysts, when choosing a comparative experiment with the amount of catalyst $[cat]_0 = 1.17$ mol.%, shows another result (Figure 7). In this case, the factor $\lambda(exp)$ was in good agreement with the ratio of the compared amounts of catalysts, Equation (7). Direct proportionality was observed between factors $\lambda(exp)$ and $\lambda(calc)$.
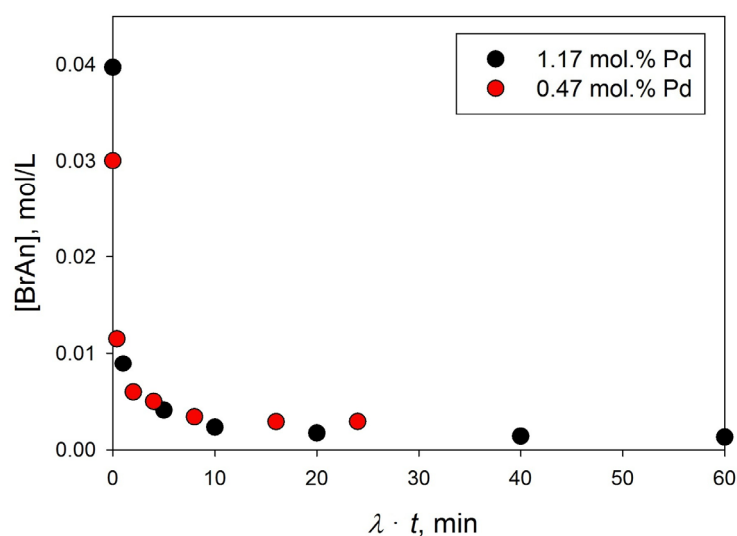
Figure 7. Dependence of the current concentration of BrAn on "conditional" reaction time in a series of experiments with different amounts of Pd(II)/HPS catalyst (black circle—1.17 mol.%, red circle—0.47 mol.%).

It is a noted feature of the kinetic curves of the reaction catalyzed by Pd(II)/HPS. Attempts to mathematically describe the generalized data in Figure 7 by classical equations of formal kinetics did not lead to the desired result, in contrast to the data in Figure 5. Nevertheless, the kinetic curves shown in both figures are well superimposed on each other, which indicates the identity of the mathematical description of the processes for each of the two catalysts. In each series of experiments, only the catalyst concentration changes. In other words, the obtained linear dependence of the factor λ(exp) vs. λ(calc) in Figures 6 and 7 indicates the first orders of the inherited reaction for each of the catalysts. When studying the Pd(0)/HPS catalyst, some of the granules formed in the pores of the support remain inaccessible to the reagents. Of course, a similar in situ Pd(II)/HPS catalyst remains available.

Therefore, we decided to analyze the data of a series of experiments on the effect of temperature and initial concentrations of the main reagent [BrAn] using the above method, of course taking into account the data just obtained.

3.3.3. Effect of Temperature

To study the effect of temperature on the reaction using the Pd(0)/HPS catalysis, a series of experiments was carried out in the temperature range of 40–70 °C with constant values of other parameters (0.47 mol.% Pd, 1 mmol BrAn, 1.5 mmol PBA, 2 mmol NaOH, EtOH/H_2O = 5:1, N_2, 800 two-sided shaking/min). This series of reactions can be viewed as a series of one-factor experiments, and a "time transformation" method similar to that used to study the effect of the amount of catalyst can be applied. In Equation (6), instead of the ratio of the amounts of catalyst, we will consider the ratio of the process rate constants (λ^*), assuming that the constant is a mathematical factor for the kinetic equation of the process and has the following form (Equation (9)):

$$\lambda^* = k_i / k_0 . \tag{9}$$

Let us choose as a comparison curve the trend line of consumption of BrAn concentration over time at 40 °C. Then, the form of kinetic curves in coordinates $[BrAn]_i$ vs. ($\lambda^* \cdot t$) can be seen in Figure 8. As can be seen from Figure 8, all data on the change in the concentration of BrAn depending on the reduced time ($\lambda^* \cdot t$) are relatively well located along the same trend line.
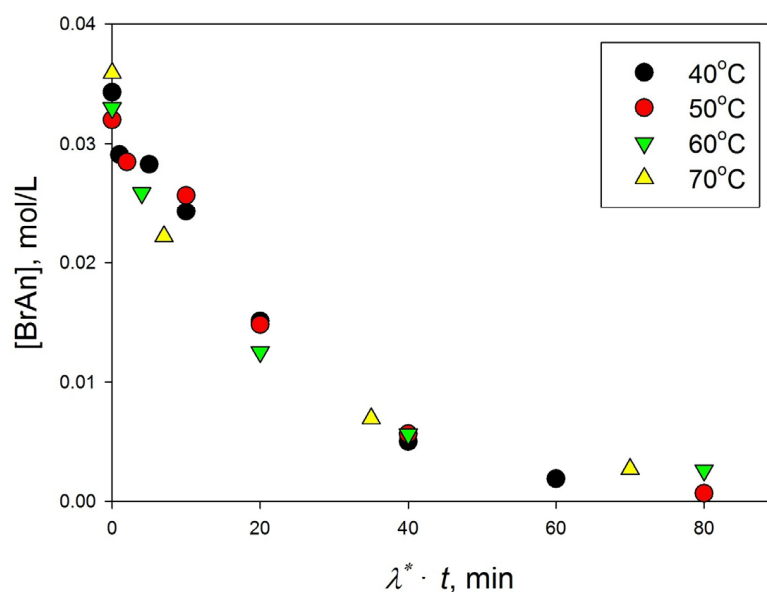
Figure 8. Consumption of BrAn at various temperatures depending on the "conditional" time (λ*·t), λ* = 1.0, 2.0, 4.0 and 7.0 for 40, 50, 60 and 70 °C, respectively.

On the one hand, this result shows that the kinetic equation for the consumption of BrAn is proportional to only one constant, which is the rate constant of the reaction at the limiting stage of the process (oxidative addition of BrAn). Of course, it should be understood that this generalized rate constant may be a combination of rate constants and equilibria for other process steps, for example, the equilibrium constant for the formation of the PBA salt (see Section 3.2).

On the other hand, from the dependence of the coefficient (λ*) on temperature, one can estimate the apparent activation energy ($E_{a,app}$) of the limiting stage (Figure 9), which is equal to 58.3 kJ/mol. This value of $E_{a,app}$ is lower in comparison with the data obtained by other research groups [41,42]: 111–116 kJ/mol for the homogeneous Suzuki cross-coupling conducted using Pd(II) carbene complex [41], and 100 kJ/mol was used for heterogeneous Pd/C [42]. We will consider the possible reason for this discrepancy when discussing the reaction mechanism.
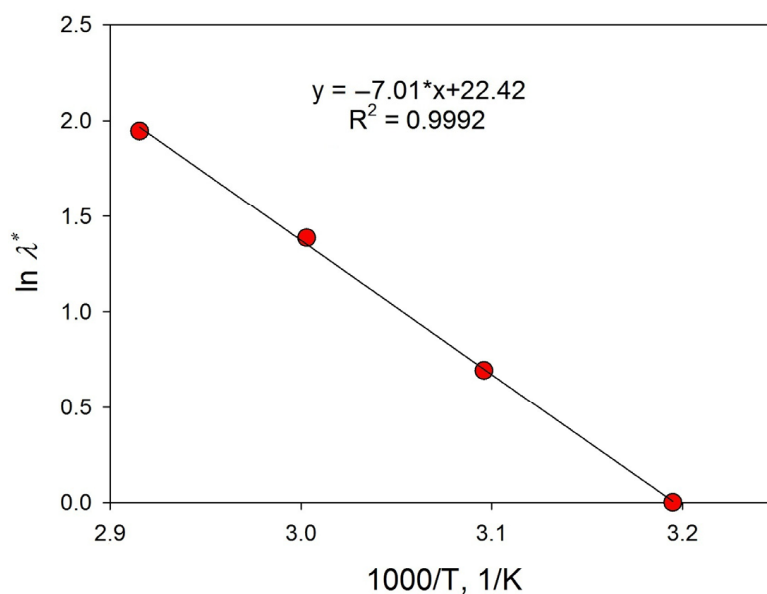

Figure 9. Arrhenius diagram for the catalyst Pd(0)/HPS.

In addition, the given method of comparing kinetic curves by transforming time makes it possible to determine a number of kinetic parameters of the process under study without knowing the exact function of the reaction rate. In this way, the first orders of the reaction with respect to the catalysts were established, and the activation energy of the rate-limiting stage of the process was determined.

Let us try to understand the information that can be obtained by considering the kinetic curves of a series of reactions with catalysts (Pd(II)·NPs) and (Pd(0)·NPs) on the effect of the initial concentrations of BrAn.

3.3.4. Influence of the Initial Concentration of BrAn

We will study the effect of the concentration of [BrAn] by another method, namely, "time shift", the essence of which consists in comparing the kinetic curves interconnected in one series of experiments by the time offset of each kinetic curve (Figure 10).
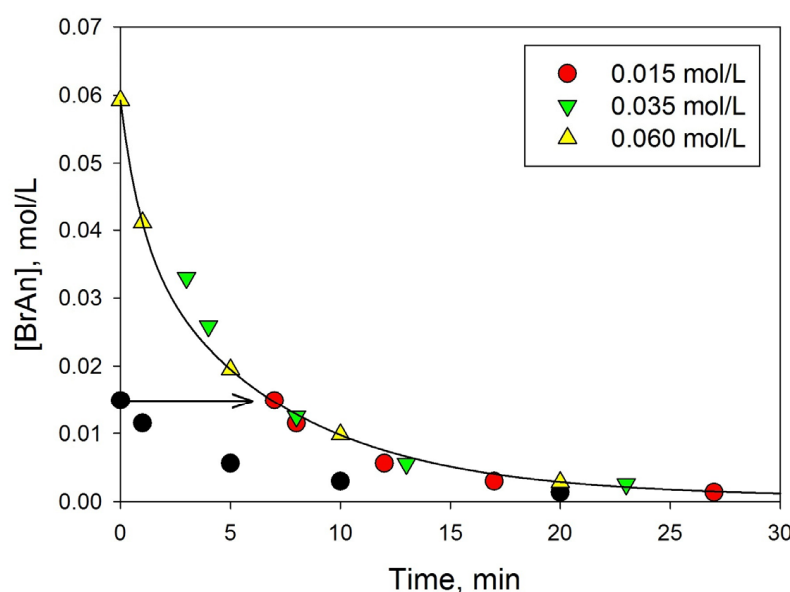

Figure 10. Dependence of the current concentration of BrAn on time in a series of experiments with different initial concentrations of $[BrAn]_0$ (yellow triangle—0.060 mol/L, green triangle—0.035 mol/L, red circle—0.015 mol/L) in the presence of Pd(0)/HPS.

On the one hand, the complete coincidence of the kinetic curves at different initial substrate concentrations, and the equality of other process parameters, may indicate the identity of the mathematical description of the compared processes [40]. We must compare the change in the course of the kinetic curve at the maximum concentration of the substrate with the experimental data of the kinetic curve with a lower initial concentration of the substrate. All other reaction parameters must match. For this purpose, we shift the time axis for the second kinetic curve until the initial concentration of the second experiment coincides with the trend line of the kinetic curve of the first experiment. At this moment, all parameters of both experiments become comparable, in addition to the fact that in the reaction mass of the first experiment, a product (or products) was formed, the concentration of which is comparable or equal to the difference in the initial concentrations of the substrates in both experiments.

On the other hand, the combination of the kinetic curves at different initial concentrations shows that the resulting product (proportional to the difference in the initial concentrations of the compared experiments) does not affect the course of the process.

In one series with Pd(0)/HPS catalysts, we change the initial concentration of the main components—BrAn, PBA and NaOH, leaving their molar ratio unchanged at 1, 1.5, and 2.0, respectively. Other process parameters also remained unchanged. For comparison, we select the trend line of the current concentrations of BrAn with its maximum initial concen-

tration $[BrAn]_0$. The values of the current concentrations $[BrAn]_i$ of all other experiments are shifted along the time axis until they fit into the trend line of the corresponding data of the comparison experiment (Figure 10).

The arrow in Figure 10 shows how the current concentrations of the experiment with an initial BrAn concentration of 0.015 mol/L (black circle) coincide with the trend line of the experiment with an initial BrAn concentration of 0.060 mol/L, on which the experimental data with an initial BrAn concentration of 0.035 mol/L are already shown. Figure 10 shows that when the current concentrations $[BrAn]_i$ are shifted for experiments with initial concentrations of 0.015 mol/L and 0.035 mol/L to the trend line of the comparison experiment, a single dependence with a single trend line is formed. In other words, the law of change in the current concentrations of BrAn at their different initial concentrations is the same.

Based on the result obtained, important conclusions can be drawn: (i) within the analysis error, the resulting products do not affect the rate of BrAn consumption; (ii) since, in the compared experiments, at the same current concentration of BrAn, the ratio of the components of $[BrAn]_i$, $[PBA]_i$, and $[NaOH]_i$ is violated, this violation does not manifest itself within the error of determination. Actually, we have already noted the weak effect of excess PBA and NaOH earlier (see Section 3.2).

In a series of experiments with Pd(II)/HPS catalysts, we obtained a completely different result (see Figure 11), although all process parameters remained the same, including the amount of palladium.
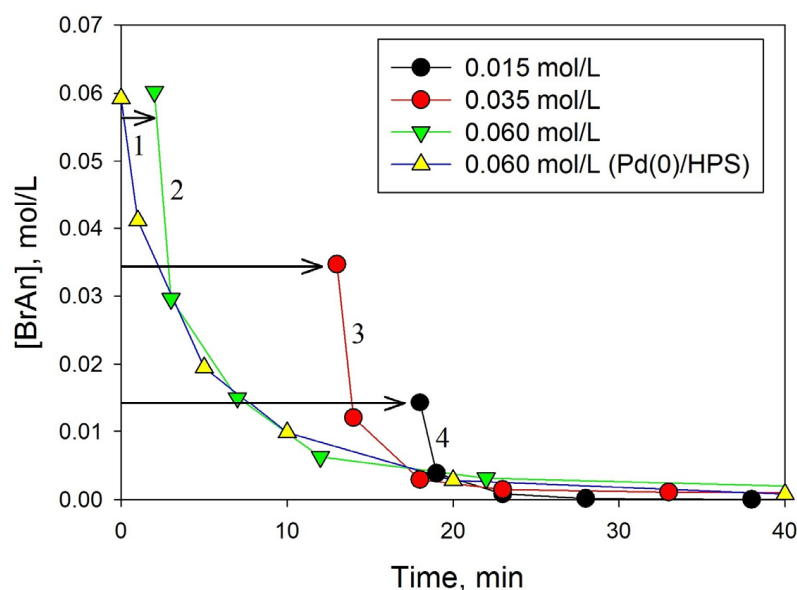

Figure 11. Dependence of the current concentration of BrAn on time in a series of experiments with different initial concentrations of $[BrAn]_0$ (green triangle—0.060 mol/L, red circle—0.035 mol/L, black circle—0.015 mol/L, curves 2, 3, and 4, respectively) in the presence of Pd(II)/HPS. Kinetic curves are shifted along the time axis by 2, 13 and 18 min, accordingly. Yellow triangles refer to the comparing kinetic curve (1) for the Pd(0)/HPS catalyst.

The initial section of the kinetic curves of dependence in the current BrAn concentration on time changed too quickly. The obtained kinetic data in the form of current concentrations of BrAn with different initial concentrations did not overlap with a shift along the time axis, especially at the beginning of the reaction. It can be assumed that the initial transition of the Pd(II)/HPS catalyst to the "hot form" occurs; the active Pd(0)/HPS catalyst is formed *in situ*.

As the reaction proceeds, that is, when the cyclic exchange of palladium Pd(II)/HPS $\leftrightarrow$ Pd(0)/HPS is stabilized, the initial form of palladium transforms into its ground state, Pd(0)/HPS, which is typical for the reduced catalyst. The transformation of the "hot"

form of the catalyst into the usual one can be seen by comparing the kinetic curves of the consumption of BrAn over time for both forms of the catalyst (Figure 11).

The data obtained under Pd(0)/HPS catalysts at the maximum initial concentration of BrAn (Figure 11, curve 1) were compared with the data obtained under Pd(II)/HPS catalysis (Figure 11, curves 2, 3, and 4). For this purpose, the current concentrations of [BrAn]i obtained for catalyst Pd(II)/HPS (Figure 11, curves 2, 3, and 4) were time-shifted so that they overlapped the trend line of the comparison experiment (Figure 11, curve 1).

When shifting the time scale for the kinetic curves of experiments with Pd(II)/HPS catalyst, only their end sections coincide with the trend line comparisons of the curve (Figure 11, curve 1), and for initial concentrations $[BrAn]_0$ = 0.060, 0.035, and 0.015 mol/L, only ≈50%, ≈15%, and ≈10% of the corresponding curve coincide with the trend line.

The coincidence of the kinetic curves at the end of the reaction for Pd(II)/HPS with the kinetic curves for Pd(0)/HPS obtained under the same process conditions indicates the same reactivity of the compared catalysts. This fact gives reason to believe that, in the initial period of the reaction under Pd(II)/HPS catalysis, this catalyst is rapidly converted to its reduced form, and the cyclic oscillation of Pd(II) ↔ Pd(0), corresponding to different forms of palladium reactions, is shifted to the right, i.e., the reaction of oxidative addition of BrAn becomes the rate-limiting stage of the process. Of course, the comparison of very low substrate concentrations for both catalysts should always be taken with caution. However, it is quite logical to assume that the high initial activity of the starting Pd(II)/HPS catalyst is associated with the activity of separate palladium atoms in the catalyst part, which are formed after the stage of reductive elimination of the Ph-Pd(II)-PhOMe fragments (Figure 1). Pd(0) atoms are still linked to the HPS matrix and are involved in two competing reactions—the formation of an oxidative addition product with continued catalytic reaction (Figure 1) and the agglomeration of palladium atoms to form nanoclusters, developing essentially in another catalyst, Pd(0)/HPS.

3.3.5. Mathematical Model of the Process and Hypothesis on the Reaction Mechanism

Considering the dependences of the course of the kinetic curves for various process conditions (in Section 3.3), we obtained extremely important conclusions about the behavior of both Pd(II)/HPS and Pd(0)/HPS catalysts in the process of Suzuki cross-coupling. In the absence of large amounts of data about the reaction catalyzed by Pd(II)/HPS, for discussion, we consider the laws of the reaction catalyzed mainly by Pd(0)/HPS catalyst.

So, we found that the reaction rate is proportional to the initial amount of available catalyst for the reactants (Figure 6). The linearity of the dependence of λ(exp) on λ(calc) indicates the first order of the reaction with respect to the catalyst. It can be concluded that the amount of unavailable palladium (blocked in the pores of the support) is the same for all the catalysts taken. The remainder of the catalyst performs its function in direct proportion to the amount of catalyst. On the other hand, as should be expected, we found that the kinetic curves of consumption of BrAn for all amounts of catalyst have the same time dependence (Figure 5) and, corrected for the amount of catalyst, merge into one. Taking into account the different reaction times, this effect of the catalyst shows that the catalyst does not change during the experiment and is a prime factor in the kinetic Equation (5).

Considering the effect of temperature, we found that this constant includes the functional dependence of the BrAn flow rate (Equation (5)) and is the effective rate constant. Its temperature dependence (apparent activation energy) is 58.3 kJ/mol. The kinetic curves of consumption of BrAn, corrected for temperature, merge into one (Figure 8), including the kinetic curves of a series of experiments on the amount of catalyst.

From a series of reactions at different initial concentrations of BrAn, we found that the kinetic curves form a single dependence in the coordinates $[BrAn]_i$ vs. time (t), if we combine the initial concentrations of the reagent with the trend line for BrAn consumption, which is selected as a comparison curve (Figure 10).

Thus, by processing the kinetic data, we obtained only one multiparametric kinetic curve for different series of experiments, which greatly facilitated the finding of a mathe-

matical model of the Suzuki-Miyaura cross-coupling reaction. In various coordinates, it is shown in Figures 5, 8 and 10.

Unfortunately, the indicated variants of the generalized curves do not correspond to the classical first-order reaction equation. At deep conversion of BrAn, the calculated curve is slightly lower than the experimental values, which would correspond to a higher order of the reaction. The simplest explanation for this is the assumption that PBA is involved in the limiting stage of the reaction. In Section 3.2, we showed that the transfer of the phenyl moiety to the palladium atom can only proceed from the PBA anion, which is formed in equilibrium from PBA and NaOH. In this case, the general picture of the process is presented to us as follows.

In the reaction medium from BrAn and Pd(0)/HPS catalyst, the oxidative addition reaction proceeds (Equation (1), Section 3.2). Parallel to this, an equilibrium reaction for the formation of PBA salt is taking place (Equation (4), Section 3.2). Further, the main reaction of exchange of negatively charged ligands proceeds (10):

$$\text{Br-Pd(II)-PhOMe} + \{\text{PhB(OH)}_3\}^- \rightarrow \text{Ph-Pd(II)-PhOMe} + \text{B(OH)}_3 + \text{Br}^-. \tag{10}$$
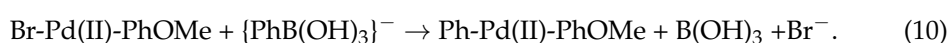
The resulting palladium complex decomposes to the final product (MBP) by the reductive elimination reaction with the regeneration of the initial Pd(0)/HPS catalyst (cat). The proposed scheme corresponds to the following mathematical description (Equations (11)–(17)).

$$\text{d[BrAn]}\big/\text{dt} = -k_1[\text{BrAn}][\text{cat}] + k_{-1}[\text{X}] \tag{11}$$

$$\text{d[PBA]}\big/\text{dt} = -k_2[\text{PBA}][\text{NaOH}] + k_{-2}[\text{Na(PhB(OH)}_3)] \tag{12}$$

$$\text{d[X]}\big/\text{dt} = k_1[\text{BrAn}][\text{cat}] - k_{-1}[\text{X}] - k_3[\text{X}] \cdot \left[(\text{PhB(OH)}_3)^-\right] \tag{13}$$

$$\text{d[Y]}\big/\text{dt} = k_3[\text{X}] \cdot \left[(\text{PhB(OH)}_3)^-\right] - k_{-4}[\text{Y}] \tag{14}$$

$$\text{d[MBP]}\big/\text{dt} = k_{-4}[\text{Y}] \tag{15}$$

$$\text{d[Na(PhB(OH)}_3)]\big/\text{dt} = k_2[\text{PBA}][\text{NaOH}] - k_{-2}[\text{Na(PhB(OH)}_3)] - k_3[\text{X}] \cdot \left[(\text{PhB(OH)}_3)^-\right] \tag{16}$$

$$\text{d}\left[\text{Br}^-\right]\big/\text{dt} = \text{d[NaBr]}\big/\text{dt} = k_3[\text{X}] \cdot \left[(\text{PhB(OH)}_3)^-\right] \tag{17}$$

where [X] and [Y] are products of oxidative addition {Br-Pd(II)-(PhOMe)} and {Ph-Pd(II)-(Ph-OMe)}, respectively.

Unfortunately, we have little experimental data to find all the kinetic parameters of the resulting system of differential equations (Equations (11)–(17)). However, we can greatly simplify the task by introducing some restrictions.

We assume that the equilibrium concentration of the formed organometallic product (X) is very low compared to the initial concentration of BrAn. Otherwise, the selectivity of the target product would be very low due to the formation of exchange products (bis-phenol or bis-anisole). On the other hand, the formation of salt from PBA acid and alkali should proceed very quickly, and, given the low acidity of PBA, the equilibrium should be shifted towards the starting substances.

If our assumptions are correct, then Equations (11) and (12) can be set equal to zero. In this case, we can obtain some important relationships (Equations (18) and (19)).

$$[\text{X}] = {}^{k_1}\big/k_{-1}[\text{BrAn}][\text{cat}] \tag{18}$$

$$[\text{Na(PhB(OH)}_3)] = {}^{k_2}\big/k_{-2}[\text{PBA}][\text{NaOH}] \tag{19}$$

In addition, summing the left and right sides of Equations (14) and (15), we obtain a simple kinetic equation (Equation (20)) formed by the total MBP ($[MBP]_{total}$), which is in solution and in combination with the catalyst.

$$d[Y]\big/dt + d[MBP]\big/dt = d[MBP]_{total}\big/dt = k_3[X]\cdot[(PhB(OH)_3)^-] \qquad (20)$$

Taking into account Equations (18) and (19), we obtain a mathematical expression for the formation of a cross-coupling product (Equation (21)):

$$d[MBP]\big/dt = k_1k_2k_3\big/k_{-1}k_{-2}[cat][BrAn][PBA][NaOH] = k_{eff}[cat][BrAn][PBA][NaOH] \qquad (21)$$

The data processing of the experimental series described above was carried out with the usual integration of Equation (21), finding the calculated BrAn concentrations, and the nonlinear least squares method for minimizing the deviations of the calculated concentration from the experimental values. The level of reliability (R^2) of the correlation between the experimental and calculated data is $R^2 = 0.97-0.99$ for the entire series of experiments in accordance with Equation (21) and the effective rate constant, which has the following form (Figure 11):

$$k_{eff} = \exp(24.6 - 58300/RT) \qquad (22)$$

It should be noted that the obtained expression (Equation (21)) for the generalized rate constant is given for the catalyst Pd(0)/HPS, taken in an amount of 0.047 mol.%, and the factor (cat) = 1. For other amounts of catalyst, this multiplier must be calculated in accordance with the expression for the trend line in Figure 6.

The complex expression for the effective rate constant (k_{eff}) explains the reason for the low apparent activation energy we obtained (i.e., 58.3 kJ/mol), since it is the algebraic sum of the activation energies of individual reactions with rate constants, which, as factors, are found in Equation (21). A good description of the experimental data by Equation (21) indicates that the limiting stage Suzuki cross-coupling reaction is the reaction of two equilibrium forming precursors ({Br-Pd(II)-(PhOMe)} and the anion of the sodium salt of PBA $[(PhB(OH)_3)^-]$) with the rate constant k_3. Said equilibriums are strongly shifted toward the starting materials.

4. Discussion

We have shown that Pd-containing HPS-based catalysts can be active and selective in the Suzuki cross-coupling between BrAn and PBA. The general mechanism of the Suzuki reaction is known from the literature; however, there is still discussion about the details. For example, in most cases, milder bases are considered more preferable due to the possible changes in the transmetalation pathway (from the hydroxo pathway to the borate pathway). In this study, we showed that the use of a stronger base (NaOH) is preferable, and moreover, the molar excess of NaOH is required, indicating that the formation of trihydroxyborate is a key step.

It should be noted that we investigated ligandless catalysts, as aromatic polymeric support (HPS) bears no functional groups capable of coordinating palladium. Thus, there are no limitations for the transformation of the catalyst morphology during the reaction (see one of our previous works [16]). Such peculiarities of ligandless catalytic systems cause difficulties in describing kinetics, as well as in proposing the reaction mechanism. In spite of this, we have postulated the rapid formation of the "hot" form of the catalyst under reaction conditions while using unreduced Pd(II)/HPS, which further underwent transformation to Pd(0)/HPS, and the cyclic oscillation of Pd(II) $\leftrightarrow$ Pd(0) was shifted to the right. Thus, oxidative addition was chosen as the rate-limiting stage of the process.

Aiming at Pd(0) as an active form, the formal kinetic approach was applied for the description of the observed experimental dependencies. Though the obtained expressions are empirical, we believe that the general approach is simple and can be applied to a wide

range of ligandless catalytic systems, resulting in a better description and understanding of cross-coupling processes.

5. Conclusions

In this work, the Suzuki cross-coupling reaction was investigated using Pd NPs embedded in an aromatic polymer matrix of HPS. It was shown that the application of the methods of "non-formal kinetics" makes it possible to analyze such difficult, multistage processes, which are catalyzed by a number of metal forms. Usually, the basis of the whole process is represented by cyclic reactions of transformation of one form of a catalyst into another: metal (0) $\leftrightarrow$ metal (II). In such cases, the function defining the change in the current substrate concentrations almost always remains unknown. The kinetic analysis technique was used to determine a set of basic process parameters describing its regularity, until the mechanism of elementary reactions occurring was established.

In fact, in the absence of knowledge of the basic law of substrate consumption, both methods can be effectively used—the method of "time transformation" and the method of "time shift". In the first case, the use of said methods allows determining the reaction order with respect to the catalyst and the apparent activation energy of the process step, which determines the reaction rate (e.g., see Sections 3.3.2 and 3.3.3). In the second case, the method of the "time shift" reveals the effect on the rate of the process, as well as the initial substrate concentration and the resulting reaction products (e.g., see Section 3.3.4). We would prefer to especially emphasize that the use of the above methods of "non-formal kinetics" is particularly fruitful and can be used to study complex multi-step processes when classical kinetics approaches are either ineffective or very labor-intensive.

Data Availability Statement: Not applicable.

Conflicts of Interest: The authors declare no conflict of interest.

References

1. Jung, J.-Y.; Taher, A.; Hossain, S.; Jin, M.-J. Highly active heterogeneous palladium catalyst for the Suzuki reaction of heteroaryl chlorides. *Bull. Korean Chem. Soc.* **2010**, *31*, 3010–3012. [CrossRef]
2. Pan, C.; Liu, M.; Zhang, L.; Wu, H.; Ding, J.; Cheng, J. Palladium Catalyzed Ligand-Free Suzuki Cross-Coupling Reaction. *Catal. Commun.* **2008**, *9*, 321–323. [CrossRef]
3. Kylmälä, T.; Tois, J.; Xu, Y.; Franzén, R. One Step Synthesis of Diflunisal Using a Pd-Diamine Complex. *Cent. Eur. J. Chem.* **2009**, *7*, 818–826. [CrossRef]
4. Liu, S.-Y.; Li, H.-Y.; Shi, M.-M.; Jiang, H.; Hu, X.-L.; Li, W.-Q.; Fu, L.; Chen, H.-Z. Pd/C as a Clean and Effective Heterogeneous Catalyst for C–C Couplings toward Highly Pure Semiconducting Polymers. *Macromolecules* **2012**, *45*, 9004–9009. [CrossRef]
5. Soomro, S.S. C-C Coupling Reactions Catalyzed by Supported Palladium in Liquid Phase. Ph.D. Thesis, Technische Universität Münc, Munich, Germany, 2009; 134p.
6. D'Alterio, M.C.; Casals-Cruañas, È.; Tzouras, N.V.; Talarico, G.; Nolan, S.P.; Poater, A. Mechanistic Aspects of the Palladium-Catalyzed Suzuki-Miyaura Cross-Coupling Reaction. *Chem. Eur. J.* **2021**, *27*, 13481–13493. [CrossRef] [PubMed]
7. Sołoducho, J.; Olech, K.; Świst, A.; Zając, D.; Cabaj, J. Recent Advances of Modern Protocol for C-C Bonds—The Suzuki Cross-Coupling. *Adv. Chem. Eng. Sci.* **2013**, *3*, 19–32. [CrossRef]
8. Devendar, P.; Qu, R.-Y.; Kang, W.-M.; He, B.; Yang, G.-F. Palladium-Catalyzed Cross-Coupling Reactions: A Powerful Tool for the Synthesis of Agrochemicals. *J. Agric. Food Chem.* **2018**, *66*, 8914–8934. [CrossRef]

9. Thomas, A.A.; Wang, H.; Zahrt, A.F.; Denmark, S.E. Structural, Kinetic, and Computational Characterization of the Elusive Arylpalladium(II)boronate Complexes in the Suzuki-Miyaura Reaction. *J. Am. Chem. Soc.* **2017**, *139*, 3805–3821. [CrossRef]

10. Yang, C.; Zhang, L.; Lu, C.; Zhou, S.; Li, X.; Li, Y.; Yang, Y.; Li, Y.; Liu, Z.; Yang, J.; et al. Unveiling the full reaction path of the Suzuki–Miyaura cross-coupling in a single-molecule junction. *Nat. Nanotechnol.* **2021**, *16*, 1214–1223. [CrossRef]

11. Somorjai, G.A. On the Move. *Nature* **2004**, *430*, 730. [CrossRef]

12. Kann, N. Recent Applications of Polymer Supported Organometallic Catalysts in Organic Synthesis. *Molecules* **2010**, *15*, 6306–6331. [CrossRef] [PubMed]

13. Liu, T.Z.; Lee, S.D.; Bhatnagar, R.S. Toxicity of Palladium. *Toxicol. Lett.* **1979**, *4*, 469–473. [CrossRef]

14. Emsley, J. *Nature's Building Blocks: An A-Z Guide to the Elements*; Oxford University Press: Oxford, UK, 2011; pp. 384–387.

15. Hosseini, M.-J.; Jafarian, I.; Farahani, S.; Khodadadi, R.; Tagavi, S.H.; Naserzadeh, P.; Mohammadi-Bardbori, A.; Arghavanifard, N. New Mechanistic Approach of Inorganic Palladium Toxicity: Impairment in Mitochondrial Electron Transfer. *Metallomics* **2016**, *8*, 252–259. [CrossRef]

16. Pagliaro, M.; Pandarus, V.; Ciriminna, R.; Béland, F.; Carà, P.D. Heterogeneous versus Homogeneous Palladium Catalysts for Cross-Coupling Reactions. *ChemCatChem* **2012**, *4*, 432–445. [CrossRef]

17. Nikoshvili, L.; Bakhvalova, E.S.; Bykov, A.V.; Sidorov, A.I.; Vasiliev, A.L.; Matveeva, V.G.; Sulman, M.G.; Sapunov, V.N.; Kiwi-Minsker, L. Study of Deactivation in Suzuki Reaction of Polymer-Stabilized Pd Nanocatalysts. *Processes* **2020**, *8*, 1653. [CrossRef]

18. Schmidt, A.F.; Kurokhtina, A.A.; Larina, E.V. Simple Kinetic Method for Distinguishing Between Homogeneous and Heterogeneous Mechanisms of Catalysis, Illustrated by the Example of "Ligand-Free" Suzuki and Heck Reactions of Aryl Iodides and Aryl Bromides. *Kinet. Catal.* **2012**, *53*, 84–90. [CrossRef]

19. Schmidt, A.F.; Kurokhtina, A.A. Distinguishing Between the Homogeneous and Heterogeneous Mechanisms of Catalysis in the Mizoroki-Heck and Suzuki-Miyaura Reactions: Problems and Prospects. *Kinet. Catal.* **2012**, *53*, 714–730. [CrossRef]

20. Kashin, A.S.; Ananikov, V.P. Catalytic C-C and C-Heteroatom Bond Formation Reactions: In Situ Generated or Preformed Catalysts? Complicated Mechanistic Picture behind Well-Known Experimental Procedures. *J. Org. Chem.* **2013**, *78*, 11117–11125. [CrossRef]

21. Eremin, D.B.; Ananikov, V.P. Understanding Active Species in Catalytic Transformations: From Molecular Catalysis to Nanoparticles, Leaching, "Cocktails" of Catalysts and Dynamic Systems. *Coord. Chem. Rev.* **2017**, *346*, 2–19. [CrossRef]

22. Reay, A.J.; Fairlamb, I.J.S. Catalytic C–H Bond Functionalisation Chemistry: The Case for Quasi-Heterogeneous Catalysis. *Chem. Commun.* **2015**, *51*, 16289–16307. [CrossRef]

23. Narayanan, R.; El-Sayed, M.A. Effect of Catalysis on the Stability of Metallic Nanoparticles: Suzuki Reaction Catalyzed by PVP-Palladium Nanoparticles. *J. Am. Chem. Soc.* **2003**, *125*, 8340–8347. [CrossRef] [PubMed]

24. Li, G.; Lei, P.; Szostak, M.; Casals-Cruañas, E.; Poater, A.; Cavallo, L.; Nolan, S.P. Mechanistic Study of Suzuki–Miyaura Cross-Coupling Reactions of Amides Mediated by [Pd(NHC)(allyl)Cl] Precatalysts. *ChemCatChem* **2018**, *10*, 3096–3106. [CrossRef]

25. Balanta, A.; Godard, C.; Claver, C. Pd Nanoparticles for C–C Coupling Reactions. *Chem. Soc. Rev.* **2011**, *40*, 4973–4985. [CrossRef] [PubMed]

26. Biffis, A.; Centomo, P.; Del Zotto, A.; Zecca, M. Pd Metal Catalysts for Cross-Couplings and Related Reactions in the 21st Century: A Critical Review. *Chem. Rev.* **2018**, *118*, 2249–2295. [CrossRef]

27. Bouleghlimat, A.; Othman, M.A.; Lagrave, L.V.; Matsuzawa, S.; Nakamura, Y.; Fujii, S.; Buurma, N.J. Halide-Enhanced Catalytic Activity of Palladium Nanoparticles Comes at the Expense of Catalyst Recovery. *Catalysts* **2017**, *7*, 280. [CrossRef]

28. Boztepe, C.; Künkül, A.; Gürbüz, N.; Özdemir, İ. The Kinetics and Mechanism of Polymer-Based NHC-Pd-Pyridine Catalyzed Heterogeneous Suzuki Reaction in Aqueous Media. *Int. J. Chem. Kin.* **2019**, *51*, 931–942. [CrossRef]

29. Mohanty, S.; Punji, B.; Maravanji, B. Synthesis and Reaction Kinetics of Pd(1,5-cyclooctadiene)Cl$_2$ with N,N′-Methylene-bis(2-aminopyridyl): An Efficient Catalyst for Suzuki-Cross-Coupling Reactions. *Polyhedron* **2006**, *25*, 815–820. [CrossRef]

30. Liu, Y.; Hartman, R.L. Reaction Kinetics of a Water-Soluble Palladium-β-Cyclodextrin Catalyst for a Suzuki-Miyaura Cross-Coupling in Continuous Flow. *React. Chem. Eng.* **2019**, *4*, 1341–1346. [CrossRef]

31. Fyfe, J.W.B.; Fazakerley, N.J.; Watson, A.J.B. Chemoselective Suzuki–Miyaura Cross-Coupling via Kinetic Transmetallation. *Angew. Chem. Int. Ed.* **2017**, *129*, 1269–1273. [CrossRef]

32. Sulman, E.M.; Nikoshvili, L.Z.; Matveeva, V.G.; Tyamina, I.Y.; Sidorov, A.I.; Bykov, A.V.; Demidenko, G.N.; Stein, B.D.; Bronstein, L.M. Palladium Containing Catalysts Based on Hypercrosslinked Polystyrene for Selective Hydrogenation of Acetylene Alcohols. *Top. Catal.* **2012**, *55*, 492–497. [CrossRef]

33. Nemygina, N.; Nikoshvili, L.; Bykov, A.; Sidorov, A.; Molchanov, V.; Sulman, M.; Tiamina, I.; Stein, B.; Matveeva, V.; Sulman, E.; et al. Catalysts of Suzuki cross-coupling based on functionalized hyper-cross-linked polystyrene: Influence of precursor nature. *Org. Process Res. Dev.* **2016**, *20*, 1453–1460. [CrossRef]

34. Adrio, L.A.; Nguyen, B.N.; Guilera, G.; Livingston, A.G.; Hii, K.K.M. Speciation of Pd(OAc)$_2$ in Ligandless Suzuki-Miyaura Reactions. *Catal. Sci. Technol.* **2012**, *2*, 316–323. [CrossRef]

35. Sherwood, J.; Clark, J.H.; Fairlamb, I.J.S.; Slattery, J.M. Solvent Effects in Palladium C$_a$talysed Cross-Coupling Reactions. *Green Chem.* **2019**, *21*, 2164–2213. [CrossRef]

36. National Institute of Standards and Technology. *NIST X-ray Photoelectron Spectroscopy Database*; Version 4.1; National Institute of Standards and Technology: Gaithersburg, MD, USA, 2012. Available online: http://srdata.nist.gov/xps/ (accessed on 21 November 2020).

37. Amatore, C.; Jutand, A.; Le Duc, G. Kinetic Data for the Transmetalation/Reductive Elimination in Palladium-Catalyzed Suzuki-Miyaura Reactions: Unexpected Triple Role of Hydroxide Ions Used as Base. *Chem. Eur. J.* **2011**, *17*, 2492–2503. [CrossRef] [PubMed]

38. Carrow, B.P.; Hartwig, J.F. Distinguishing between Pathways for Transmetalation in Suzuki−Miyaura Reactions. *J. Am. Chem. Soc.* **2011**, *133*, 2116–2119. [CrossRef] [PubMed]

39. Schmidt, A.F.; Kurokhtina, A.A.; Larina, E.V. Role of a base in Suzuki-Miyaura reaction. *Russ. J. Gen. Chem.* **2011**, *81*, 1573–1574. [CrossRef]

40. Schmid, R.; Sapunov, V. *Non-Formal Kinetics: In Search for Chemical Reaction Pathways (Monographs in Modern Chemistry)*, 14th ed.; Wiley-VCH Verlag GmbH: Weinheim, Germany, 1982; 199p.

41. Polynski, M.V.; Ananikov, V.P. Modeling Key Pathways Proposed for the Formation and Evolution of "Cocktail"-Type Systems in Pd-Catalyzed Reactions Involving ArX Reagents. *ACS Catal.* **2019**, *9*, 3991–4005. [CrossRef]

42. Collins, G.; Schmidt, M.; O'Dwyer, C.; Holmes, J.D.; McGlacken, G.P. The Origin of Shape Sensitivity in Palladium-Catalyzed Suzuki-Miyaura Cross Coupling Reactions. *Angew. Chem. Int. Ed.* **2014**, *53*, 4142–4145. [CrossRef]